Modal interferometer based on hollow-core photonic crystal fiber for strain and temperature measurement

S. H. Aref[1,2,*], R. Amezcua-Correa[3], J. P. Carvalho[1,4], O. Frazão[1,4], P. Caldas[1,4,5], J. L. Santos[1,4], F. M. Araújo[1], H. Latifi[2], F. Farahi[6], L. A. Ferreira[1], J. C. Knight[3]

[1]*INESC Porto, Rua do Campo Alegre, 687, 4169-007 Porto, Portugal*
[2]*Laser and Plasma Research Institute, University of Shahid Beheshti, Evin,Tehran, Iran*
[3]*Department of Physics, University of Bath, Claverton Down, Bath, BA2 7AY, UK*
[4]*Dept. de Física da Faculdade de Ciências da Universidade do Porto, Rua do Campo Alegre 687, 4169-007 Porto, Portugal.*
[5]*Escola superior de Tecnologia e Gestão de Viana do Castelo, Av. do Atlântico, Apartado 574, 4900-348 Viana do Castelo, Portugal*
[6]*Department of Physics and Optical Science, University of North Carolina at Charlotte, Charlotte, NC 28223, USA*
**h-aref@cc.sbu.ac.ir*

Abstract: In this work, sensitivity to strain and temperature of a sensor relying on modal interferometry in hollow-core photonic crystal fibers is studied. The sensing structure is simply a piece of hollow-core fiber connected in both ends to standard single mode fiber. An interference pattern that is associated to the interference of light that propagates in the hollow core fundamental mode with light that propagates in other modes is observed. The phase of this interference pattern changes with the measurand interaction, which is the basis for considering this structure for sensing. The phase recovery is performed using a white light interferometric technique. Resolutions of ± 1.4με and ± 0.2°C were achieved for strain and temperature, respectively. It was also found that the fiber structure is not sensitive to curvature.

OCIS codes: (230.3990) Microstructure devices; (120.3180) Interferometry; (060.2370) Fiber optics sensors; (060.5295) Photonic crystal fibers.

References and links

1. R. Thapa, K. Knabe, K. L. Corwin, and B. R. Washburn, "Arc fusion splicing of hollow-core photonic bandgap fibers for gas-filled fiber cells," Opt. Express **14**(21), 9576–9583 (2006).
2. W. N. MacPherson, M. J. Gander, R. McBride, J. D. C. Jones, P. M. Blanchard, J. G. Burnett, A. H. Greenaway, B. Mangan, T. A. Birks, J. C. Knight, and P. St. J. Russell, "Remotely addressed optical fibre curvature sensor using multicore photonic crystal fibre," Opt. Commun. **193**(1-6), 97–104 (2001).
3. C.-L. Zhao, L. Xiao, J. Ju, M. S. Demokan, and W. Jin, "Strain and temperature characteristics of a long-period grating written in a photonic crystal fibre and its application as a temperature-insensitive strain sensor," J. Lightwave Technol. **26**(2), 220–227 (2008).
4. W. N. MacPherson, E. J. Rigg, J. D. C. Jones, V. V. Ravi, K. Kumar, J. C. Knight, and P. St. J. Russell, "Finite-element analysis and experimental results for a microstructured fibre with enhanced hydrostatic pressure sensitivity," J. Lightwave Technol. **23**(3), 1227–1231 (2005).
5. C. M. Smith, N. Venkataraman, M. T. Gallagher, D. Müller, J. A. West, N. F. Borrelli, D. C. Allan, and K. W. Koch, "Low-loss hollow-core silica/air photonic bandgap fibre," Nature **424**(6949), 657–659 (2003).
6. R. Amezcua-Correa, F. Gèrôme, S. G. Leon-Saval, N. G. R. Broderick, T. A. Birks, and J. C. Knight, "Control of surface modes in low loss hollow-core photonic bandgap fibers," Opt. Express **16**(2), 1142–1149 (2008).
7. D. Ethonlagi, and M. Zavrsnik, "Fiber-optic microbend sensor structure," Opt. Lett. **22**(11), 837–839 (1997).
8. E. Li, "Sensitivity-enhanced fiber-optic strain sensor based on interference of higher order modes in circular fibers," IEEE Photon. Technol. Lett. **19**(16), 1266–1268 (2007).
9. S. M. Tripathi, A. Kumar, R. K. Varshney, Y. B. P. Kumar, E. Marin, and J. P. Meunier, "Strain and Temperature Sensing Characteristics of Single-Mode-Multimode-Single-Mode Structures," J. Lightwave Technol. **27**(13), 2348–2356 (2009), http://apps.isiknowledge.com/full_record.do?product=UA&colname=WOS&search_mode=CitingArticles&qid=3&SID=P1o7dcma8l7khK142BM&page=1&doc=1.

#115795 - $15.00 USD Received 17 Aug 2009; revised 26 Sep 2009; accepted 27 Sep 2009; published 1 Oct 2009

10. E. Li, X. Wang, and C. Zhang, "Fiber-optic temperature sensor based on interference of selective higher-order modes," Appl. Phys. Lett. **89**(9), 091119 (2006).
11. Q. Li, C.-H. Lin, P.-Y. Tseng, and H. P. Lee, "Demonstration of high extinction ratio modal interference in a two-mode fiber and its applications for all-fiber comb filter and high-temperature sensor," Opt. Commun. **250**(4-6), 280–285 (2005).
12. J. L. Villatoro, V. P. Minkovich, and D. Monzón-Hernández, "Compact modal interferometer built with tapered microstructured optical fiber," IEEE Photon. Technol. Lett. **18**(11), 1258–1260 (2006).
13. J. Villatoro, V. P. Minkovich, V. Pruneri, and G. Badenes, "Simple all-microstructured-optical-fiber interferometer built via fusion splicing," Opt. Express **15**(4), 1491–1496 (2007).
14. H. Y. Choi, M. J. Kim, and B. H. Lee, "All-fiber Mach-Zehnder type interferometers formed in photonic crystal fiber," Opt. Express **15**(9), 5711–5720 (2007).
15. Y. Jung, H. Y. Choi, M. J. Kim, B. H. Lee, and K. Oh, "Ultra-compact Mach-Zehnder interferometer using hollow optical fiber for high temperature sensing," in Optical Fiber Communication Conference and Exposition and The National Fiber Optic Engineers Conference, OSA Technical Digest (CD) (Optical Society of America, 2008), paper JThA10.
16. T. P. Hansen, J. Broeng, C. Jakobsen, G. Vienne, H. R. Simonsen, M. D. Nielsen, P. M. W. Skovgaard, J. R. Folkenberg, and A. Bjarklev, "Air-guiding photonic bandgap fibers: Spectral properties, macrobending loss, and practical handling," J. Lightwave Technol. **22**(1), 11–15 (2004).
17. F. Benabid, F. Couny, J. C. Knight, T. A. Birks, and P. S. J. Russell, "Compact, stable and efficient all-fibre gas cells using hollow-core photonic crystal fibres," Nature **434**(7032), 488–491 (2005).
18. L. M. Xiao, M. S. Demokan, W. Jin, Y. P. Wang, and C. L. Zhao, "Fusion splicing photonic crystal fibers and conventional single-mode fibers: microhole collapse effect," J. Lightwave Technol. **25**(11), 3563–3574 (2007).
19. Y. J. Rao, and D. A. Jackson, "Review article: Recent progress in fibre-optic low-coherence interferometry," Meas. Sci. Technol. **7**(7), 981–999 (1996).
20. P. Caldas, P. A. S. Jorge, F. M. Araujo, L. A. Ferreira, M. B. Marques, G. Rego, and J. L. Santos, "Fibre modal Michelson interferometers with coherence addressing and heterodyne interrogation," Opt. Eng. **47**(4), 044401 (2008).

1. Introduction

The development of sensors based on hollow-core photonic crystal fibers (HC-PCF) has been a recent and active research topic in the context of fiber optic sensing. Particularly relevant is the application of these fibers for gas sensing in face of the large overlap of the optical field with the measurement volume [1], but other measurands have also been considered, for example bend and shape [2], strain and temperature [3], as well as hydrostatic pressure [4]. The potential benefits of guiding light in air drive from lower Rayleigh scattering, lower nonlinearity and, in principle, lower transmission loss compared to what happens in conventional waveguides [5].

HC-PCF are made with hundreds of periodically spaced air holes in a silica matrix, typically arranged in a triangular lattice, using the photonic band gap concept to propagate light inside the air-core. These fibers are usually multi-mode waveguides supporting, besides the fundamental core mode, higher order core modes, cladding modes and surface modes [5,6]. However, the attenuation of the different types of modes varies substantially and after propagation along a long length of fiber only the fundamental core mode subsists. The multi-mode operation of short lengths of HC-PCFs brings the possibility to build up modal interferometers with characteristics potentially interesting to perform optical fiber sensing.

Recently, new hybrid structures have been introduced to form fiber modal interferometers. For example, in a single mode – multimode – single mode fiber structure it was examined the effect of modal interference on the performance of a microbend sensor [7], as well as when considering strain [8,9] and temperature [9,10] measurement. Another interesting configuration was based on the series combination of single mode – two modes – single mode fiber sections, which generates a transmission interference pattern with high extinction ratio [11]. This type of interferometers has been also explored in the general context of photonic crystal fibers (PCF). Indeed, a configuration based on tapering an index-guiding PCF was suggested for an in-line variable attenuator and strain sensor, where the complete collapse of the air holes around the fiber core originates a region of solid unclad multimode fiber [12,13]. Other approach to implement modal interferometry is by doing a lateral offset in the SMF-PCF splice point to excite higher order modes in the index-guiding fiber [14]. A recently reported technique is based on the partial collapse of the air hole at a limited region of a PCF to couple light to higher modes, and it was used for strain measurement in conditions of very

#115795 - $15.00 USD Received 17 Aug 2009; revised 26 Sep 2009; accepted 27 Sep 2009; published 1 Oct 2009

high temperature in view of the thermal characteristics of fused silica fibers [14]. Also, a modal Mach-Zehnder structure in hollow-core fiber with standard single-mode input and output fibers was proposed and characterized for high-temperature sensing [15].

In this work, a fiber optic modal interferometer based on HC-PCF was studied and its characteristics for strain and temperature sensing were investigated, as well as for curvature. The readout of the interferometric phase was achieved combining white light addressing with pseudo-heterodyne signal processing.

2. Sensing principle

The sensor was fabricated using a piece of HC-PCF directly spliced between two lengths of single mode fiber (SMF-28^{TM}). A 7-cell HC-PCF with a low-loss transmission band centered at 1550 nm and a core diameter of ≈16μm was used. Figure 1, shows an optical microscope image of this fiber and its transmission characteristics in the light injection conditions in which the experiments were performed. The developed sensing head uses the effect of modal interference at the exit of the HC-PCF to achieve the measurement functionality. Indeed, when light travels through the single mode fiber and is injected into the HC-PCF the fundamental core mode and other modes are excited. After propagation of these modes in the HC-PCF, they become recombined at the exit single mode fiber. This simple configuration is similar to an all-fiber Mach-Zehnder modal interferometer with two coupling points in series, different from what is most usual when considering in-line fiber interferometers which show a Fabry-Perot structure. Therefore, when light is injected into the input single mode fiber, it is expected to observe interference fringes at the output single mode fiber. It should be noticed that the fringes are not related to the collapse of air channels of the HC-PCF, like tapering in the fusion splice point and/or broadening of fundamental mode in this region, as reported in literature [13]. In order to confirm this, some experiments were carried out to check if the fringes still appear with butt coupling instead of fusion splicing. The results obtained showed that the formation of the interference fringes is independent of the coupling method, but the amplitude of the effect is dependent on the coupling conditions. Indeed, it was also found that the amplitude of the fringes (interference visibility) can be substantially reduced by proper adjustment of the input SMF and the HC-PCF in the junction region, which actually is not necessarily the condition for optimum power coupling. The analysis of the results obtained point out for an important role of the HC-PCF cladding modes in the operation of this modal interferometer, but further theoretical and experimental studies are required for a detailed understanding of the exact type of modes involved in this interferometric structure.

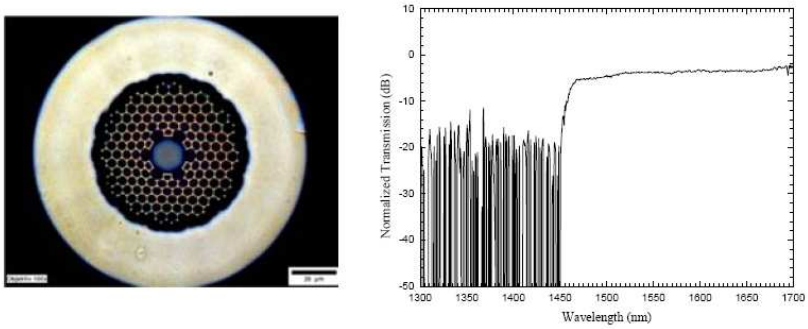

Fig. 1. Cross section photograph of a 7 cell HC-PCF (left) and normalized spectral transmission of ~1 m of this fiber spliced to a SMF28 illuminating fiber (right; the oscillations at lower wavelengths are artifacts due to the normalization).

Figure 2 shows the splice structure (in the X and Y directions) between the SMF-28 and HC-PCF fibers, as well as the observed output channeled spectrum for a piece of HC-PCF with a length of 27.8 cm. It can be observed that besides the typical two-wave interferometric behavior, there is also fringe amplitude modulation, indicating the presence of more than two

#115795 - $15.00 USD Received 17 Aug 2009; revised 26 Sep 2009; accepted 27 Sep 2009; published 1 Oct 2009

mode interference. The refractive index difference associated with the observed fringe periodicity in the figure can be calculated by means of the relation:

$$n_{eff}^{FM} - n_{eff}^{Other\ Modes} = \frac{\lambda_1 \lambda_2}{L(\lambda_1 - \lambda_2)}$$

Here, n_{eff}^{FM} and $n_{eff}^{Other\ Modes}$ are, respectively, the effective refractive index of the fundamental core mode and the average value of the effective refractive indexes of the other modes predominantly excited in the experiment performed. Also, λ_1 and λ_2 are the wavelengths corresponding to two adjacent intensity maxima and L is the length of HC-PCF. It was found that the value of $\Delta n_{eff} = n_{eff}^{FM} - n_{eff}^{Other\ Modes}$ is around 0.016, independently of L.

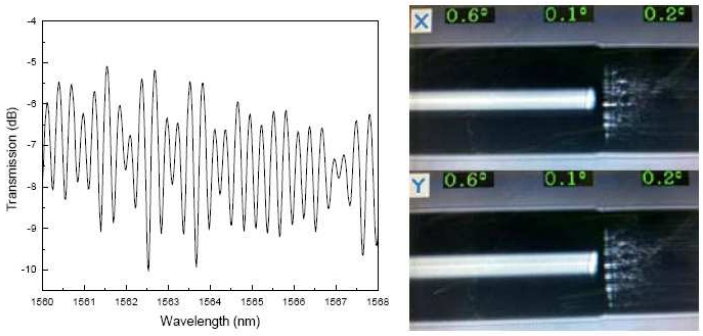

Fig. 2. Left: Channeled spectrum of the interferometric sensing head; Right: Visualization of the SMF-28/HC-PCF splice in the Fujikura's SM-40 screen.

3. Experimental Setup and Results

The initial experimental set up is shown in Fig. 3. A superluminescent Er-doped fiber ASE (amplified spontaneous emission) source, operating at 1550 nm, with a FWHM (full width at half maximum) of 60 nm and output power of 1.8 mW was used to illuminate the concatenated fibers. The HC-PCF was spliced in both ends to single mode fibers applying general procedures described elsewhere [1,16–18]. The standard machine Fujikura SM40 was used and after a training process a splice loss of ≈1.5 dB was achieved. In order to evaluate the dependence of the fringe visibility with the HC-PCF length, sensing heads with lengths of 5.1 cm, 11.6 cm, 21.4 cm and 58.8 cm were fabricated and the associated channeled spectra analyzed. For the first three lengths the visibility was around 50%, but when the longer fiber length was considered the visibility showed a substantial decrease to ≈36%. This behavior is compatible with a visibility reduction due to power loss in the higher order modes originated by a weak propagation guidance of these modes in the fiber.

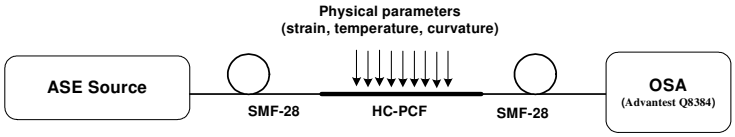

Fig. 3. Experimental setup for initial characterization of the modal interferometer.

In order to investigate the strain, temperature and curvature characteristics of the sensing head, two micro-positioners were used to fix the SMF fibers and to apply strain and curvature to the HC-PCF. For temperature characterization a furnace was used. The length of the HC-PCF was ~28 cm and the fringe visibility was found to be ~55%. Figure 4 shows the strain and temperature wavelength responses of the sensing head obtained by monitoring the shift of the channeled spectrum under the measurand action. The interferometric fringes were linearly

#115795 - $15.00 USD Received 17 Aug 2009; revised 26 Sep 2009; accepted 27 Sep 2009; published 1 Oct 2009

shifted toward shorter wavelengths with the increase of strain or temperature, with slopes of −0.96 pm/με and −7.1 pm/°C, respectively. These sensitivity values can be compared with those of a conventional single mode-multimode-single mode structure which are −2.3 pm/με and −15 pm/°C [8,10]. Concerning curvature, no measurable sensitivity was noticed, which is indeed as expectable result. The core of the fiber follows the fiber neutral line and, therefore, the optical path of the core mode is essentially curvature independent. On the other hand, the cladding modes integrate along propagation positive and negative variations in their optical path induced by the presence of curvature in the fiber, which means the net effect shall be residual. Therefore, this argument points out to an insensitivity of the sensing head to curvature.

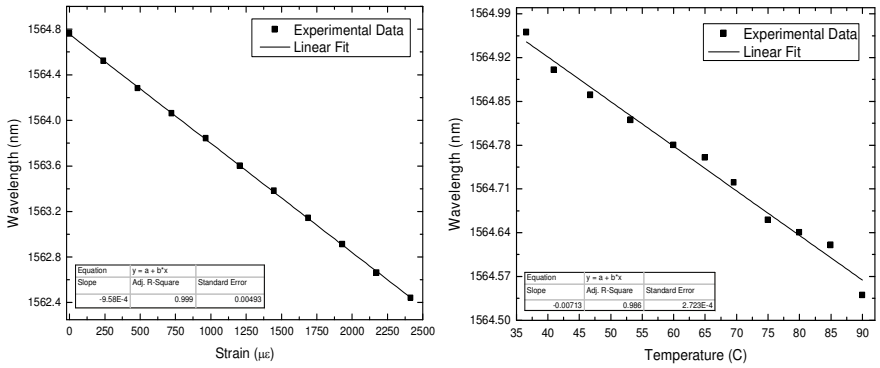

Fig. 4. Wavelength responses of the sensing head for variations of applied strain and temperature.

The blue shift of the channeled spectrum associated with the increase of temperature and strain can be understood with the following argument. Considering temperature, the thermal expansion implies a longer propagation length for the cladding modes when the temperature increases, but similar to the longer propagation length of the core mode, i.e., an increase in temperature shall originate for this type of fiber, and in view of the differential operation of the interferometer, a residual shift of the channeled spectrum due to the thermal expansion effect. The same does not happen when the thermo-optic effect is considered. The experimental results indicate its contribution is associated with the decrease of the absolute value of Δn_{eff} .To understand this, we need to consider what happens with the core mode and cladding modes involved in the modal interferometer operation when temperature increases. Because the core mode propagates essentially in air, its effective refractive index is close to one and residually sensitive to temperature variations. Therefore, the variation of Δn_{eff} is essentially associated with the temperature behaviour of the cladding modes. These modes have a substantial fraction of their optical field that propagates in silica. It is known that silica has a positive thermo-optic coefficient, therefore considering only this effect the effective refractive index of these modes would increase with temperature, leading to a larger absolute value of Δn_{eff} and, consequently, to a red shift of the channeled spectrum, contrary to what is observed. However, the situation is more complex because the optical field of these cladding modes propagates also in the air of the core/cladding holes, and the thermal expansion can induce changes in the mode fraction that propagates in the silica and in the air, with a net effect that leads to a decrease with temperature of the effective modal refractive index. Certainly this is a complex phenomenon that needs further theoretical/experimental studies for its detailed understanding.

Concerning strain, the experimental results indicate the contribution to the variation of Δn_{eff} associated with the elasto-optic effect is dominant relatively to the direct expansion effect. This is understandable considering the refractive index of silica decreases with strain,

#115795 - $15.00 USD Received 17 Aug 2009; revised 26 Sep 2009; accepted 27 Sep 2009; published 1 Oct 2009

with the consequence that the effective refractive index of the cladding modes decreases with the increase of strain. Having in mind that the effective index of the core mode is essentially unaffected by strain, the net effect is a reduction of the absolute value of Δn_{eff} originating a blue shift of the channeled spectrum with the increase of applied strain.

To measure the phase changes in the fiber modal interferometer, a second interferometer was built to implement coherence reading [19]. Figure 5 shows the setup implemented. The second interferometer is a conventional fiber Michelson interferometer with an open air path in one of its arms, which is adjusted to match the optical path difference of the sensing interferometer. The fiber in the other arm of this interferometer is wrapped around a ring-shaped piezoelectric transducer that is modulated with an electrical sawtooth waveform whose amplitude is adjusted to obtain a signal at the photodetection suitable for pseudo-heterodyne processing. After an adequate electronic filtering, this signal has the form of an electric carrier (90 Hz) with a phase that mirrors the optical phase of the tandem interferometric system. This pseudo-heterodyne processing technique is known to provide sensitive interferometric phase reading [20].

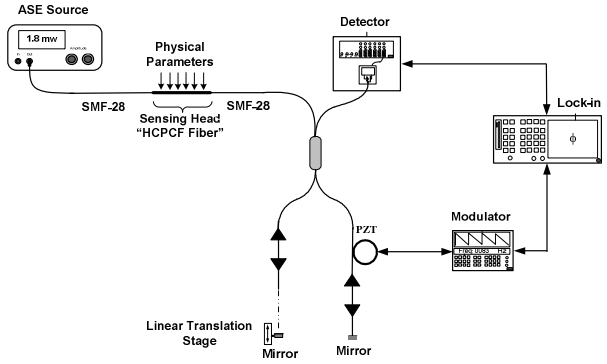

Fig. 5. Scheme of the experimental setup for phase reading with white light interferometry.

Figure 6 shows the phase changes associated with strain and temperature variations applied to the sensing head, now with L ≈32 cm and with an interferometric visibility of ~49%. Following the behavior represented in Fig. 4, the sensitivity is constant in the measurement range considered, with values of 0.76°/με and 8.1°/°C for strain and temperature, respectively.

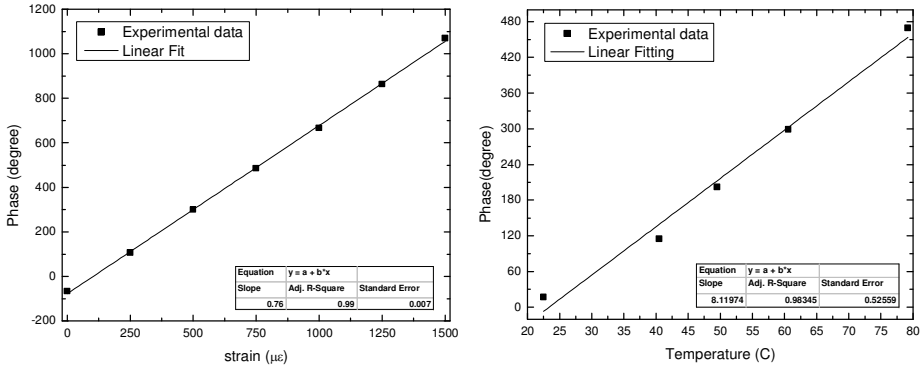

Fig. 6. Phase changes induced by strain and temperature variations applied to the sensing head.

To evaluate the measurand resolutions achievable with this sensing head structure the step technique was used (Fig. 7). If $\delta\varphi$ is the phase *rms* fluctuations during the periods of constant measurand values, and if a measurand step change ΔX ($X \rightarrow$ strain or temperature)

#115795 - $15.00 USD Received 17 Aug 2009; revised 26 Sep 2009; accepted 27 Sep 2009; published 1 Oct 2009

originates a phase step change of $\Delta\phi$, then the measurand resolution, δX is given by $\delta X = \delta\phi(\Delta X/\Delta\phi)$. For the case of temperature, in the determination of $\delta\varphi$ it was privileged the region corresponding to water at a stable temperature of 22.5°C, because it revealed difficult to stabilize the water temperature at 40.5°C after the step change, i.e., for some time the temperature of water continued to increase at a slow rate. Following this approach, resolutions of ± 1.4με and ± 0.2°C were obtained for strain and temperature, respectively.

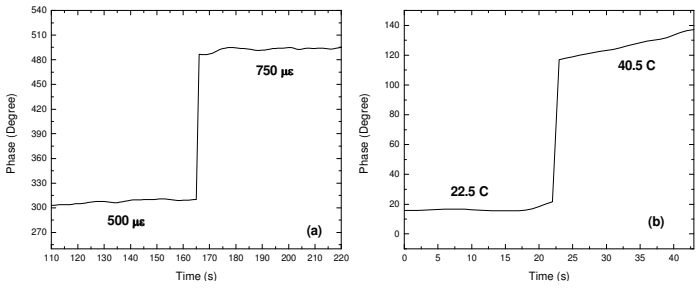

Fig. 7. Phase response of the sensing head implemented with HC-PCF fiber for a step change in (a) strain and (b) temperature.

The pseudo-heterodyne technique used to interrogate the interferometric system can be implemented with standard electronics (or using an approach relying on computer-based virtual instrumentation), which means that besides the demonstration of the proposed sensing structure, a step further was done towards the utilization of this configuration in field applications.

4. Conclusions

A sensing head based on hollow-core photonic crystal fiber for measurement of strain and temperature has been presented. The sensor consists of a piece of 7-cell HC-PCF connected to SMF-28 in both ends. The interference occurs between the fundamental mode and higher order modes inside the HC-PCF. A white light interferometric technique for coherent phase reading was used. Resolutions of ± 1.4με and ± 0.2°C were obtained for strain and temperature, respectively. It was also found that the fiber structure is not sensitive to curvature.

Acknowledgments

The authors acknowledge the R&D environment provided by the FP6 Project NextGenPCF (IST – 34918: *Next Generation Photonic Crystal Fibers*).

#115795 - $15.00 USD Received 17 Aug 2009; revised 26 Sep 2009; accepted 27 Sep 2009; published 1 Oct 2009